Submitted to Physical Review

UCRL-19754
Preprint

c. 2

REGGE-POLE MODEL FOR pp AND $\bar{p}p$ ELASTIC SCATTERING

RECEIVED
LAWRENCE
RADIATION LABORATORY
OCT - 8 1970
LIBRARY AND
DOCUMENTS SECTION

Donald M. Austin, William H. Greiman
and William Rarita

April 20, 1970

AEC Contract No. W-7405-eng-48

TWO-WEEK LOAN COPY

This is a Library Circulating Copy which may be borrowed for two weeks. For a personal retention copy, call Tech. Info. Division, Ext. 5545

UCRL-19754 c. 2

LAWRENCE RADIATION LABORATORY
UNIVERSITY of CALIFORNIA BERKELEY

3/a

DISCLAIMER

This document was prepared as an account of work sponsored by the United States Government. While this document is believed to contain correct information, neither the United States Government nor any agency thereof, nor the Regents of the University of California, nor any of their employees, makes any warranty, express or implied, or assumes any legal responsibility for the accuracy, completeness, or usefulness of any information, apparatus, product, or process disclosed, or represents that its use would not infringe privately owned rights. Reference herein to any specific commercial product, process, or service by its trade name, trademark, manufacturer, or otherwise, does not necessarily constitute or imply its endorsement, recommendation, or favoring by the United States Government or any agency thereof, or the Regents of the University of California. The views and opinions of authors expressed herein do not necessarily state or reflect those of the United States Government or any agency thereof or the Regents of the University of California.

REGGE-POLE MODEL FOR pp AND $\bar{p}p$ ELASTIC SCATTERING AT HIGH ENERGIES

Donald M. Austin, William H. Greiman, and William Rarita

Lawrence Radiation Laboratory
University of California
Berkeley, California

April 20, 1970

ABSTRACT

High energy data for pp and $\bar{p}p$ elastic scattering are confronted with the simple Regge-pole model in an attempt to discover which features of this data, if any, are beyond the power of this model. The simplest representation, with only three poles (P, P', and ω), gives a reasonable fit to all the data except the "dip" structure in the $\bar{p}p$ DCS. Several types of parameterizations were tested, including various ghost-killing mechanisms, and all produced comparable fits. To account for the $\bar{p}p$ DCS structure, and simultaneously circumvent the factorization difficulties caused by the universal zero in the ω amplitude, a fourth pole (the ω') was introduced. The four-pole parameterizations (several were tested) provide adequate fits to all the data, including the $\bar{p}p$ DCS structure, and in addition come much closer to satisfying the sum rule constraints imposed, through factorization, by the πN and KN analyses.

For completeness, another vacuum-type pole (the P") is introduced and five-pole fits parameterized as in cut models are compared with pure pole models. The results are somewhat ambiguous, showing that the high energy differential and total cross sections, polarization, ratio of real to imaginary, and Serpukhov slope data all together are still not sufficient for determining the differences between many possible parameterizations.

I. INTRODUCTION

Several recent experiments on proton-proton and antiproton-proton elastic scattering indicate some new features of these reactions which were not predicted very accurately by previous Regge-pole fits.[1] Among the features requiring modification of the old fits are the positive polarization near the forward direction for both reactions, the high energy total cross section and slope measurements from Serpukhov, and the structure in the differential cross sections (DCS) seen for $-t \approx 0.6\ (\mathrm{GeV}/c)^2$ (see Sec. II for references). Many authors have obtained fits to some of these features by introducing absorptive cuts or other modifications of simple Regge-pole theory. It is our purpose here to investigate precisely which features of the data, if any, are not amenable to the simple Regge-pole representation of the scattering amplitudes. To this end we have attempted several parameterizations conforming to the criteria of simple Regge-pole theory--i.e., parameters restricted to the more or less accepted values associated with the trajectory and residue functions established by previous analyses considering finite energy and continuous moment sum rules (FESR and CMSR), the resonance spectrum, and factorization.

In Sec. II we describe the data used in the analysis, and Sec. III gives a brief description of our parameterization of the amplitudes and observables. Section IV is devoted to fits using only the three well-known isoscalar Regge trajectories P, P', and ω, which give an adequate description of most of the data, but seem incapable of describing some important features. In Sec. V we attempt to improve

the fits as well as circumvent the factorization difficulties of the ω residue function by introducing a secondary ω-type contribution with several different parameterizations. The rather ambiguous results obtained from this process lead us to Sec. VI, wherein all caution is abandoned and five-pole fits are investigated. The five-pole parameterizations are seen to provide excellent fits to all the data, including the structure seen in the latest experiments, with reasonable but nonunique values of the parameters. The discussion of the significance of the various fits is pursued in Sec. VII.

II. DESCRIPTION OF THE DATA

A. Cross-Section Data

Several interesting experiments done since the RRCP fits[1] invite a new interpretation of the structure seen in elastic N-N cross-section data. Of particular interest are the $\bar{p}p$ total cross sections[2] and the slope measurements of the pp DCS,[3] which extend the lab momentum range under consideration to 70 GeV/c. This wide range of lab momentum allows much more precision in the determination of the energy dependence, and therefore, the Regge trajectories. Some high-precision DCS data have become available recently which show interesting structure in the Regge region. The $\bar{p}p$ DCS at 8.0 and 16.0 GeV/c[4] indicate a shoulder, or the remnants of a dip occurring at lower energies, near $-t = 0.6\ (\mathrm{GeV/c})^2$. New pp DCS data at 19.2 and 21.1 GeV/c[5] show a definite flattening effect for $-t > 1.0\ (\mathrm{GeV/c})^2$. These two features pose severe constraints on the residue functions.

B. Polarization Data

Perhaps the most interesting of the new data are the polarization data at 6.0 GeV/c for pp and $\bar{p}p$,[6] and the 14.0-GeV/c data for pp.[7] The precision of these new data is critical for determining structure of residue functions, such as the sign of the helicity-flip terms and ghost-killing mechanisms.

The 6.0-GeV/c pp polarization has distinctive dips near $-t = 0.6$ and $0.9\ (\mathrm{GeV/c})^2$, and a large ($\approx 25\%$) bump near $-t = 1.25\ (\mathrm{GeV/c})^2$. The 14.0-GeV/c data, on the other hand, dip to $\approx -10\%$ at $-t = 1.25\ (\mathrm{GeV/c})^2$, indicating a rather drastic energy dependence at

large $-t$ that places severe constraints on the parameters. Also, since the $\bar{p}p$ polarization at 6.0 GeV/c is positive for $-t < 0.3$ $(\text{GeV/c})^2$, the mechanism producing this polarization cannot be P-ω interference, as previously conjectured,[1] since the pp and $\bar{p}p$ data have the same sign for small t and, moreover, do not vanish at the crossover point, $-t \approx 0.13$ $(\text{GeV/c})^2$.

C. Ratio of Real to Imaginary and Slope Data

The data on the ratio of the real to the imaginary part of the forward scattering amplitude, taken as a whole, are inconsistent. Rather than favor one experiment over another or attempt to juggle systematic errors, we simply used the data as published. This means that a χ^2 of 3 or 4 per point is the best one can expect for a fit. Our fits reflect this fact, while producing reasonable agreement with the overall trend of the data to decrease in magnitude with increasing energy.

The pp DCS slope data[3] were taken in the range $0.008 \leq -t \leq 0.12$ $(\text{GeV/c})^2$, for p_{lab} from 13.0 to 69.9 GeV/c. Since these data do not coincide with the other DCS data in this energy range,[8] we scaled the data by the systematic error quoted by the experimenters, ± 0.3 (actually, we multiplied the data by a scale factor of 0.97, which amounts to very nearly the same thing). With the exception of the point at $p_{lab} = 63.5$ GeV/c, which is somewhat higher than the other points and invariably produced a χ^2 of 10 to 20, we were able to obtain fits with a χ^2 of 1 per point or so with nearly all parameterizations. Hence, our feeling is that these data produced little difficulty for the Regge-pole representation of the scattering amplitudes. As for

determining the slope of the pomeron trajectory, it is very important to consider the range of energy involved as well as the aberrations of the data. For example, if one takes the two points at $p_{lab} = 27.5$ and 69.9 GeV/c, one finds $\alpha'_P = \left[\frac{\Delta \text{ slope}}{2 \ln(s_2/s_1)}\right] = 0.33 \text{ (GeV/c)}^{-2}$; selecting the two points at $p_{lab} = 13.0$ and 63.5 GeV/c gives $\alpha'_P = 0.7 \text{ (GeV/c)}^{-2}$. Although the first value appears to have been determined in a more reasonable manner, one should be hesitant about ignoring other choices. The data are simply not good enough to decide such fine points.

D. Summary

Below is summarized our selection of data used in the fits:[9]

$\frac{d\sigma}{dt}$ (238 points):	p_{lab}
pp	6.8, 8.8, 10.8, 12.8, 14.8, 16.7, 19.6, 21.9, 24.6;[10] 19.2, 21.1;[5]
$\bar{p}p$	7.2, 8.9, 10.0, 11.8, 12.0;[10] 8.0, 16.0;[4]
σ_T (28 points):	
pp	6.0 to 22.0,[11] 7.8 to 26.0,[12] 10.1, 19.3, 26.4;[13]
$\bar{p}p$	6.0 to 22.0,[11] 20.0 to 50.0;[2]
Polarization (99 points):	
pp	5.9, 7.0,[14] 6.0,[6] 10.0, 12.0,[15] 14.0;[7]
$\bar{p}p$	6.0;[6]

(Continued)

(Cont.)

Re/Im (15 points):	p_{lab}
pp	7.8 to 26.2,[12] 10.1, 19.3, 26.4,[13] 24.0,[16] 7.85,[17] 10.0;[18]
$\bar{p}p$	11.9;[12]
Slope (20 points):	
pp	13.0 to 69.9.[3]

III. KINEMATICS AND NOTATION

Our notation is adapted from RRCP,[1] with a few minor changes. Only terms of first order in $\cos\theta_t$ have been kept, and we parameterize the t-channel helicity amplitudes and use them directly in the expressions for observables. Ignoring unnatural parity contributions, such as π, A_1, etc., we find three t-channel helicity amplitudes (free of kinematic singularities and parity conserving) which we parameterize as follows:

$$\Phi_1 = \Phi_2 = \sum_i \xi_i \, f_{ss}{}^i(t) \, \nu^{\alpha_i(t)} ,$$

$$\Phi_3 = -\Phi_4 = -\sum_i \xi_i \, f_{nn}{}^i(t) \, \nu^{\alpha_i(t)} ,$$

$$\Phi_5 = \sum_i \xi_i \, f_{sn}{}^i(t) \, \nu^{\alpha_i(t)} ,$$

where $\nu = (s - u)/4M^2$ and

$$\xi_i = -\pi^{-1}\{\pm 1 + \exp[-i\,\pi\,\alpha_i(t)]\}\,\Gamma[1 - \alpha_i(t)] ,$$

$$f_{ss}{}^i(t) = (1 - t/4M^2)[b_s{}^i \exp(c_s{}^i t)]^2 \, g_{ss}{}^i ,$$

$$f_{nn}{}^i(t) = \frac{-t/4M^2}{1 - t/4M^2}\,[b_n{}^i \exp(c_n{}^i t)]^2 \, g_{nn}{}^i ,$$

$$f_{sn}{}^i(t) = (-t/4M^2)^{\frac{1}{2}} \, b_s{}^i \, b_n{}^i \exp[(c_s{}^i + c_n{}^i)t] \, g_{sn}{}^i ,$$

and the g's are the various ghost-killing mechanisms which satisfy the equation $g_{ss}{}^i \, g_{nn}{}^i = (g_{sn}{}^i)^2$.

The signature factors ξ_i contain an extra factor of α in the numerator, which is compensated for in defining the ghost-killing factors; i.e., we have used the relation

$$(\pi\,\alpha)^{-1}\,\Gamma(1-\alpha) = [\sin \pi\alpha \times \Gamma(1+\alpha)]^{-1} .$$

The units of the Φ's are mb-GeV/c, so the b's are in $(\text{mb-GeV/c})^{\frac{1}{2}}$, the c's are in $(\text{GeV/c})^{-2}$, and the expressions for the observables are

$$\sigma_T = p_{lab}^{-1}\,\text{Im}\,\Phi_1 \quad (t=0) ,$$

$$\frac{d\sigma}{dt} = (0.226/p_{lab})^2\,\{|\Phi_1|^2 + |\Phi_3|^2 + 2|\Phi_5|^2\} ,$$

$$P = \frac{-2\,\text{Im}\{\Phi_5^*[\Phi_1 + \Phi_3]\}}{\{|\Phi_1|^2 + |\Phi_3|^2 + 2|\Phi_5|^2\}} ,$$

$$\text{Re/Im} = \text{Re}\,\Phi_1(t=0)/\text{Im}\,\Phi_1(t=0)$$

$$\text{slope} = \left[\ell n\,\frac{d\sigma}{dt}\,(t=-0.064) - \ell n\,\frac{d\sigma}{dt}\,(t=-0.065)\right]/0.001 .$$

The factor $0.226 = \dfrac{(\text{mb})^{\frac{1}{2}}\,\text{GeV}}{4(\pi)^{\frac{1}{2}}\,\hbar\,c}$ is the usual conversion factor to mb/GeV^2 for the DCS, including an extra constant factor, $(16\pi)^{-\frac{1}{2}}$.

These expressions are equivalent to those used in RRCP except for the factor of 2 in the expression for the polarization (which was inadvertently omitted in writing the formula in that paper, but not in their calculation).

The ghost-killing factors appropriate for this form of ξ_i are:

	Sense	Chew	Gell-Mann	No compensation
g_{ss}	$1/\alpha$	1	1	α
g_{nn}	α	α^2	1	α
g_{sn}	1	α	1	α

The kinematic factors differ from those given by Wang[19] only in terms like $(1 - t/4M^2)$, which are unimportant in the region of interest. We chose to retain the factors used in RRCP for comparison purposes.

IV. THREE-POLE FITS

A. General Features

In the spirit of RRCP,[1] the data were confronted with the simplest of Regge devices--viz., the three isoscalar trajectories P, P', ω. Contributions from isovector exchange, such as π, ρ, and A_2, can be estimated from the np and $\bar{p}p$ charge-exchange cross sections to be smaller than the isoscalar contributions by at least an order of magnitude, and are ignored in this initial gambit for a simple representation of the data.

Due to the well-known factorization difficulty concerning the zero in the ω residue functions at the crossover point (see Sec. V), the ω contribution must be considered as representing an effective negative-parity amplitude which vanishes near $t = -0.13\ (\mathrm{GeV}/c)^2$ to account for the crossover phenomenon. The residues for the three-pole fits were parameterized by setting $b_{s,n}^{P,P'}$ = constant, $b_s^{\omega} = (1 - t/t_0)^{\frac{1}{2}} \times$ constant, and $b_n^{\omega} = (1 - t/t_0)^{\frac{1}{2}} \times$ constant, as required by factorization. Thus, the interpretation is that the P' and ω represent effective Regge contributions of positive and negative parity respectively, while the P represents the Pomeranchuk contribution. The deviation of the parameters from "canonical"[20] values then serves as some vague measure of the non-simple-Regge-pole content of the parameterization.

From the several varieties of parameterization tested, including various ghost-killing mechanisms and sign combinations of the helicity-flip residues, the following general features emerge:

(a) A generally good fit to all the pp DCS data, including the flattening seen in the 19.2- and 21.1-GeV/c data for $1.2 \leq -t \leq 2.3$ $(\mathrm{GeV/c})^2$;

(b) a concomitant inability to simultaneously reproduce the dips in the 8.0- and 16.0-GeV/c $\bar{p}p$ DCS near $t = -0.8$ $(\mathrm{GeV/c})^2$ (however, the fits for smaller $-t$ are generally good);

(c) surprisingly good fits to the Serpukhov pp slope and $\bar{p}p$ total cross section data, with a pomeron slope of about 0.35 $(\mathrm{GeV/c})^{-2}$;

(d) polarization fits with χ^2 per point exceeding 2, but with vastly different shapes for different parameterizations.

These features were common to all parameterizations that produced reasonable fits (say, with χ^2 per point less than 2) to the data sample. The agreement for $-t < 0.6$ $(\mathrm{GeV/c})^2$ was very good--all the trouble is caused by large $-t$ structure.

B. Signs of Helicity-Flip Residue Functions

In terms of total χ^2, the relative signs of the b_n's could not be determined. Only in the shape of the polarization can one sign combination be distinguished from another. Although some combinations were able to reproduce the dip-bump structure of the 6.0-GeV/c pp polarization data, none of the three-pole fits could reproduce the strong energy dependence seen for $-t > 1.0$ $\mathrm{GeV/c}^2$, and all combinations gave a χ^2 of more than 2 per point for the polarization. Taking as a guideline that the three-pole parameterization should be able to reproduce the small $-t$ structure, such as the positive values for both pp and $\bar{p}p$ polarization and the dip near $-t = 0.6$ $(\mathrm{GeV/c})^2$,

we fitted all the data except polarization with the various sign combinations and compared the predicted polarization from these parameters. The features found were [using the notation sign (b_n^P), sign $(b_n^{P'})$, sign (b_n^{ω})] as follows:

(a) When freed from the constraints of polarization fitting, all combinations wanted rather drastic small $-t$ behavior, presumably to better match the larger slope of the DCS data in that region:

(b) Only the combinations $(+ + +)$, $(+ + -)$, $(- + +)$, and $(- + -)$ give positive polarization for both pp and $\bar{p}p$ in the small $-t$ region.

(c) The last two combinations, with sign $(b_n^P) = -$, predict negative pp polarization for $-t > 0.4$ $(\mathrm{GeV}/c)^2$, contrary to fact:

(d) The combinations $(+ + +)$ and $(+ + -)$ both seem to reproduce the general shape of the 6.0-GeV/c data, including the large bump for $-t$ near 1.2 $(\mathrm{GeV}/c)^2$. From this we conclude that sign (b_n^P) = sign $(b_n^{P'}) = +$, that sign (b_n^{ω}) is not well determined by this method, and that secondary contributions are necessary to reproduce the energy dependence seen in the large $-t$ polarization data.

Moreover, the conclusions seem to hold for the several combinations of ghost-killing mechanisms tried, as discussed in the next section.

C. Ghost-Killing Mechanisms

Recent analyses of low-energy πN[21] and KN[22] data using continuous-moment sum rules (CMSR) indicate that the mechanism preferred by P and P' in those reactions is the no-compensation mechanism,

whereas the ω seems to prefer the sense-choosing mechanism. One observation can immediately be made--that is, if the P' contribution vanishes, as required by the no-compensation mechanism when $\alpha_{P'} = 0$, then the $\bar{p}p$ polarization at that point will be of opposite sign to the pp polarization and 5 to 10 times as large in the energy region considered here. This effect is due to the large anti-shrinking slope of the $\bar{p}p$ DCS and to the fact that the ω contribution changes sign between the two expressions. If the dip in the pp data at $-t \approx 0.6$ $(\mathrm{GeV/c})^2$ is a reflection of $\alpha_{P'} = 0$, then $P_{\bar{p}p}$ at $p_{lab} = 6.0$ GeV/c and $-t \approx 0.6\,(\mathrm{GeV/c})^2$ should be $-10\,P_{pp}$ at the same point, which is 0.052 ± 0.019--i.e., the no-compensation mechanism gives $P_{\bar{p}p} \approx -50\%$ there. Some data in this region would help determine whether the P' contribution should vanish or not, and thus help pin down the ghost-killing mechanisms applicable to NN scattering.

Using the abbreviations S = sense-choosing, C = Chew, G = Gell-Mann, and N = no-compensation, we present a comparison of fits using several different combinations of ghost-killing mechanisms:

P	P'	ω	χ^2
N	N	S	715
N	N	C	708
C	C	S	778
G	G	G	732

From these results one can conclude that, although the vanishing of the P' seems to give a slightly better fit, the data really do not determine

a mechanism. The parameters for the NNS fit, which agree with the features seen in CMSR and FESR applied to πN[21] and KN[22] data, were perhaps the most reasonable representation of all the data It should also be noted that all these fits gave a similar prediction for $\bar{p}p$ polarization; i.e., $P_{\bar{p}p}$ is positive near the forward direction and large and negative ($\approx -50\%$) around $-t = 0.6\ (\mathrm{GeV}/c)^2$. In the case of the NNS and NNC fits, it seems reasonable that the vanishing of the P' contribution, where $\alpha_{P'} = 0$, leads to P-ω interference of equal and opposite magnitude. Since $d\sigma/dt$ for $\bar{p}p$ is on the order of only one fifth to one tenth of that for pp, the $\bar{p}p$ polarization should be 5 to 10 times as large in magnitude as the pp polarization. This must happen in any three-pole fit in which the P' contribution vanishes. However, it is somewhat of a mystery why the CCS and GGG fits, in which the P' contribution does not vanish, have structure very similar to the NNC and NNS fits. The phase cancellations must be somehow demanded by the data in such a way as to produce effective cancellation of the P-P' terms near $-t = 0.6\ (\mathrm{GeV}/c)^2$.

In Table I we have presented two examples of three-pole fits, both of the NNS variety--i.e., the P and P' have the no-compensation mechanism and the ω has the sense-choosing mechanism. Fit #1 has only the P intercept fixed (at 1.0), and fit #2 has, in addition, the slope of the P' fixed at 1.0. In both fits, the ω trajectory emerged as rather flat, indicating that the difference between pp and $\bar{p}p$ data falls off somewhat more slowly at large $-t$ than a canonical

ω trajectory would allow. The second fit is shown in Figs. 1-4 where it is seen that the $\bar{p}p$ DCS at $-t \approx 0.8\ (\mathrm{GeV}/c)^2$ is inadequately represented, as is the large $-t$ energy dependence of the polarization. Other features seem to be reasonably fitted.

Table I. Three-pole fit parameters for NNS parameterization. Fit #1 has only $\alpha_P = 1.0$ fixed; fit #2 has, in addition, $\alpha'_{P'} = 1.0$ fixed.

		α_0	α'	b_s	c_s	b_n	c_n	t_0
Fit #1	P	1.0[a]	0.35	5.8	1.6	0.97	-0.7	-
	P'	0.67	1.64	7.4	0.1	51.5	8.9	-
	ω	0.45	0.60	4.5	1.7	-31.0	3.5	0.13
Fit #2	P	1.0[a]	0.36	5.8	1.6	1.0	-0.8	-
	P'	0.67	1.0[a]	7.5	1.9	54.8	8.9	-
	ω	0.44	0.56	4.6	1.7	-25.4	3.7	0.13

	$\frac{d\sigma}{dt}$	σ_T	P	$\frac{Re}{Im}$	Slope	χ^2	Number of parameters
Fit #1	362	32	224	67	30	715	18
Fit #2	415	26	219	67	33	760	17
Number of data points	238	28	99	15	20	Total = 400 data points	

a. Fixed.

V. FOUR-POLE FITS

A. General Features

The factorization problems associated with the incorporation of a universal zero in the ω residue functions are well known. This zero, which explains the crossover in DCS for pp and $\bar{p}p$, as well as for K^+p and K^-p, does not appear in $\pi N \to \rho N$,[23] or in $\gamma p \to \pi^0 p$,[24] as factorization requires. Thus there must exist another contribution to the same amplitudes, the ω', to circumvent these problems as well as the disagreement between the analyses of $\pi N \to \rho N$[23] and KN FESR[22,25] on the existence of a nonsense zero in the helicity-flip coupling at $-t = 0.5\ (\mathrm{GeV}/c)^2$.

To obtain the zero in the negative-parity amplitudes as a cancellation between two Regge poles, ω and ω', we considered two forms: (a) $\Phi_\omega + t\,\Phi_{\omega'}$, and (b) $\Phi_\omega - \Phi_{\omega'}$. It is evident that the cancellation zero will be energy dependent unless $\alpha_\omega(t) = \alpha_{\omega'}(t)$, and a cursory analysis of the data convinces one that only a very mild energy dependence of the crossover point in KN and NN DCS will be tolerated by the data. In general, we found that $\alpha_\omega(0) \approx \alpha_{\omega'}(0)$ was a necessity, whereas some difference in slopes was possible. Also, the four-pole fits were able to fit the shoulder in the $\bar{p}p$ DCS while simultaneously fitting the rest of the data as well as or better than the three-pole fits. Hence we conclude that the introduction of an ω' contribution, required a priori by factorization, provides a reasonable fit to all the pp and $\bar{p}p$ elastic data above $p_{lab} = 6.0$ GeV/c and for $-t < 2.5$ $(\mathrm{GeV}/c)^2$. However, we must also conclude that uniqueness is not a

quality of these fits any more than it was for the three-pole case. Adequate fits were obtained with either form (a) or (b), and with trajectories fixed to resemble cuts or fixed to enforce weak exchange degeneracy between the P' and ω. The best fits, in terms of minimum χ^2, have rather perplexing parameters which tend to obscure rather than enlighten. All fits discussed below have the no-compensation mechanism for P and P' and the sense-choosing mechanism for the ω and ω'.

B. The Form $\Phi_\omega + t\,\Phi_{\omega'}$

In Table II we display the parameters for three different fits having the form $\Phi = \Phi_P + \Phi_{P'} + \Phi_\omega + t\,\Phi_{\omega'}$. Fit #1 has only $\alpha_P(0) = 1.0$ fixed, and gives $\chi^2/N = 576/400$, considerably better than the three-pole fit. A physical interpretation of the ω and ω' trajectories would certainly be entertaining, but we are unprepared to speculate at present.

Fit #2 has $\alpha'_\omega = 1.0$ and $\alpha'_{\omega'} = 0.5$ fixed in addition, which allows a possible interpretation of the ω' as a P-ω cut (ignoring the $\ln s$ behavior, of course). This seems to have mainly spoiled the polarization fit, jacking up χ^2 to 709.

Finally, fit #3 has $\alpha_\omega(t) = \alpha_{\omega'}(t) = \alpha_{P'}(t) = 0.5 + 0.9\,t$, and gives $\chi^2 = 703$. Thus the cut interpretation (fit #2) certainly isn't forced upon us by this data. Some interpretations of two ω's with the same trajectories appearing in NN scattering exist, but these are better left to their proponents for publicity. We simply state here that the data are compatible with such an interpretation.

Table II. Parameters for four-pole fits of the form $\Phi = \Phi_P + \Phi_{P'} + \Phi_\omega + t\,\Phi_{\omega'}$. In all fits the P and P' have the no-compensation mechanism and the ω and ω' have the sense-choosing mechanism.

		α_0	α'	b_s	c_s	b_n	c_n
Fit #1	P	1.0[a]	0.32	6.0	1.7	3.3	0.3
	P'	0.63	0.98	7.4	8.7	56.6	2.7
	ω	0.49	0.53	4.3	0.5	-125.1	8.0
	ω'	0.58	0.74	10.4	1.0	9.1	0.0
Fit #2	P	1.0[a]	0.31	5.5	1.7	3.1	0.3
	P'	0.70	1.20	7.6	2.0	38.1	3.6
	ω	0.39	1.0[a]	5.0	1.3	-7.0	0.0
	ω'	0.39	0.5[a]	12.9	1.8	30.9	0.6
Fit #3	P	1.0[a]	0.37	6.2	1.8	2.6	-0.1
	P'	0.5[a]	0.9[a]	9.1	8.9	74.0	2.7
	ω	0.5[a]	0.9[a]	4.1	-0.3	-123.0	7.8
	ω'	0.5[a]	0.9[a]	11.5	0.6	2.0	-0.9

	$\frac{d\sigma}{dt}$	σ_T	P	$\frac{Re}{Im}$	Slope	χ^2	Number of parameters
Fit #1	335	39	102	64	36	576	23
Fit #2	333	32	236	69	39	709	21
Fit #3	403	59	134	68	39	703	17
Number of data points	238	28	99	15	20	Total = 400 data points	

a. Fixed.

C. The Form $\Phi_\omega - \Phi_{\omega'}$

In Table III are displayed the parameters for fits having the form

$$\Phi = \Phi_P + \Phi_{P'} + \Phi_\omega - \Phi_{\omega'} .$$

This is the simplest form for producing a cancellation, and is perhaps easier to interpret in terms of dipoles, cuts, or something worse. As before, we give the readers three choices of trajectories to speculate upon; as before, the results are similarly confusing.

Fit #1 has only the P intercept fixed and the results seem fairly close to exchange degeneracy for the trajectories. The χ^2 of 588 is competitive with that in Sec. B, and there is little to distinguish between the two forms in the results.

Fit #2 has $\alpha'_\omega = 1.0$ and $\alpha'_{\omega'} = 0.5$, which pushes the χ^2 up to 661, mainly due to the polarization fit. This is the fit displayed in Figs. 5-8 where it can be seen that all the data are adequately represented by a four-pole fit with reasonable values of the parameters.

Fit #3 with degenerate trajectories is equivalent to breaking factorization for the ω, and simultaneously including more complicated residue functions. In this fit, $\Phi_\omega^{ss} - \Phi_{\omega'}^{ss} = 0$ at $t = -0.17\ (\mathrm{GeV}/c)^2$, $\Phi_\omega^{nn} - \Phi_{\omega'}^{nn} = 0$ at $t = -0.31\ (\mathrm{GeV}/c)^2$, and $\Phi_\omega^{sn} - \Phi_\omega^{sn} \neq 0$. This is in qualitative agreement with the KN FESR results,[22] in which the non-flip coupling seems to vanish at a different value of t from the flip coupling.

Table III. Parameters for four-pole fits of the form $\Phi = \Phi_P + \Phi_{P'} + \Phi_\omega - \Phi_{\omega'}$. In all fits the P and P' have the no-compensation mechanism and the ω and ω' have the sense-choosing mechanism.

		α_0	α'	b_s	c_s	b_n	c_n
Fit #1	P	1.0[a]	0.30	5.6	1.8	2.3	0.1
	P'	0.71	1.03	7.3	6.4	54.7	3.8
	ω	0.60	1.15	5.9	1.9	-35.8	1.2
	ω'	0.70	0.92	3.9	0.4	5.1	-0.6
Fit #2	P	1.0[a]	0.29	5.7	1.9	3.0	0.4
	P'	0.67	0.97	7.7	4.7	62.1	4.3
	ω	0.41	1.0[a]	8.2	1.5	-13.2	0.5
	ω'	0.40	0.5[a]	6.6	1.0	28.0	0.4
Fit #3	P	1.0[a]	0.38	6.2	1.8	2.5	-0.1
	P'	0.5[a]	0.9[a]	9.1	9.5	87.8	2.9
	ω	0.5[a]	0.9[a]	8.3	1.4	-77.2	9.2
	ω'	0.5[a]	0.9[a]	7.2	0.5	3.4	-0.9

	$\frac{d\sigma}{dt}$	σ_T	P	$\frac{Re}{Im}$	Slope	χ^2	Number of parameters
Fit #1	302	20	175	57	34	588	23
Fit #2	305	32	222	67	35	661	21
Fit #3	421	56	152	74	43	746	17
Number of data points	238	28	99	15	20	Total = 400 data points	

a. Fixed.

D. Summary

The tables of parameters are meant to illustrate the nonuniqueness of Regge fits of NN elastic data as well as the adequacy of the Regge pole representation. There need to be further restrictions on the residue functions, such as those provided by sum rules for πN and KN scattering. The relation $A' \approx \nu B$, predicted by sum rules for P and P',[21,22] should, by factorization, imply the relations

$$b_s^P \exp(c_s^P t) \approx b_n^P \exp(c_n^P t) \quad \text{and}$$

$$b_s^{P'} \exp(c_s^{P'} t) \approx b_n^{P'} \exp(c_n^{P'} t) .$$

For the four-pole fits the relation is fairly well satisfied for the P, but not for the P'.

For completeness, some fits were tried with the $(1 - t/t_0)$ factor in the ω amplitudes, i.e., the form $(1 - t/t_0)\,\Phi_\omega + \Phi_{\omega'}$ was used. This form was apparently unable to reproduce the structure in the $\bar{p}p$ DCS and was therefore not investigated further.

VI. FIVE-POLE FITS

Since the sum rule calculations[21] seem to require yet another vacuum contribution, dubbed the P", some varieties of five-pole fits were tried. As expected, such a parameterization leads to rampant ambiguity, and the only way to obtain results with even a modicum of interest is to fix some of the trajectory parameters. We define a trajectory with (a) a slope near 0.5 $(\mathrm{GeV}/c)^{-2}$, (b) whose amplitude occurs with a negative sign (relative to like contributions) to be "cut-like" (as opposed to the usual, or "pole-like" parameterization). Symbolically, a fit with the P" and ω' treated as "cut-like" will be indicated by $P + P' - P'' + \omega - \omega'$, etc. In general, the five-pole fits gave $\chi^2 < 600$, and most varieties of parameterization produced fits which were indistinguishable from the others. The ω' preferred to remain "cut-like," as it must in order to provide the weakly energy-dependent crossover zero in the DCS. The P" gave equally good fits with "cut-like" or "pole-like" parameters. These statements refer to fits in which the slopes of P' and ω were held fixed at 0.9 or 1.0. In Table IV we list some parameters as examples of five-pole fits. We emphasize that there is nothing unique about these parameters--there exist many other sets that produce adequate fits to the data, including "cut-like" forms as well as "pole-like" forms, various ghost-killing mechanisms, and other variations. For example, residue functions of the form $\beta = \exp(-0.5\ i\ \pi\alpha)[b \exp(ct)]$ produced fits competitive with the gamma-function forms in Sec. III.

Table IV. Parameters for various forms of five-pole fits. The NNNSS and GGGGG refer to the ghost-killing mechanisms, and the form of the amplitudes is indicated for each fit.

		α_0	α'	b_s	c_s	b_n	c_n
Fit #1	P	1.0[a]	0.26	6.0	2.0	2.1	0.0
NNNSS	P'	0.65	1.0[a]	7.1	6.5	72.0	10.3
(P + P' + P" + ω + t ω')	P"	-0.21	0.5[a]	15.1	2.7	-98.0	2.6
	ω	0.52	1.0[a]	4.3	5.5	-88.8	1.6
	ω'	0.38	0.5[a]	9.0	1.4	19.4	0.6
Fit #2	P	1.0[a]	0.36	5.8	1.6	1.3	-0.5
NNNSS	P'	0.60	0.9[a]	9.9	3.5	71.3	5.4
(P + P' - P" + ω - ω')	P"	0.34	0.5[a]	9.9	0.5	38.3	8.1
	ω	0.41	0.9[a]	9.6	1.6	-29.5	1.7
	ω'	0.40	0.5[a]	8.4	1.3	20.5	0.3
Fit #3	P	1.0[a]	0.25	5.7	2.0	1.1	-0.2
GGGGG	P'	0.68	0.9[a]	6.2	6.2	51.2	5.9
(P + P' - P" + ω - ω')	P"	-0.21	0.5[a]	3.0	-0.3	-4.5	-0.8
	ω	0.45	0.9[a]	14.0	1.0	-29.6	1.5
	ω'	0.45	0.5[a]	11.9	1.3	2.9	0.4

a. Fixed.

(Continued)

Table IV. (Continued)

	$\frac{d\sigma}{dt}$	σ_T	P	$\frac{Re}{Im}$	Slope	χ^2	Number of parameters
Fit #1	286	18	82	69	47	502	25
Fit #2	308	24	144	63	40	579	25
Fit #3	303	25	124	61	46	561	25
Number of data points	238	28	99	15	20	Total = 400 data points	

Fit #1 in Table IV has the form $P + P' + P'' + \omega + t\,\omega'$, with the vacuum poles all having the no-compensation mechanism and the ω's having the sense-choosing mechanism. The P intercept and the slopes of the other poles were held fixed. This fit is shown in Figs. 9-12.

Fit #2 has the form $P + P' - P'' + \omega - \omega'$, and has the same ghost killers as fit #1. The difference of 77 in χ^2 is probably not significant.

Fit #3 also has the form $P + P' - P'' + \omega - \omega'$, but here all poles have the Gell-Mann ghost-killing mechanism. The difference between the fits is noticeable only in the prediction of the $\bar{p}p$ polarization, which is somewhat larger for small $-t$ and smaller in magnitude for intermediate $-t$ for this parameterization than for the others. However, since the data are hardly sufficient to determine the behavior in this region, no preference can be voiced for any version of parameterization.

VII. DISCUSSION

In summary several points of interest emerge:

1. The three-pole parameterization is inadequate, mainly because of the failure to fit the structure in the $\bar{p}p$ DCS.
2. The four-pole parameterization, even when restricted to a factorization-breaking form that really only need involve the addition of one additional parameter over the three-pole form, is capable of giving a reasonable representation of all the data. However, the data, which are some of the best high-energy data in existence, do not distinguish between various possible parameterizations.
3. Five-pole fits, without the use of sum rule constraints, are non-unique and probably not very useful.

Some fits were tried on a combination of $\pi^{\pm}p$ elastic and charge exchange, $K^{\pm}p$ elastic and charge exchange, and the above pp and $\bar{p}p$ elastic data, obtained by using the usual P, P', ρ, A_2, and ω and enforcing factorization. Our preliminary conclusions are that fits with $\chi^2/\text{point} \approx 3$ can be obtained to all the above data together with reasonable parameters. Incompatability of the many data sets involved seems to be more responsible for the bad fit than inadequacies of the simple Regge pole model. Since it is very difficult to assure oneself that all these experiments have no normalization errors with respect to each other, factorization constraints do not seem to be the answer to obtaining unique fits. The most positive statement that can be made is that the present NN data certainly cause no embarassment for simple Regge-pole theory (or for some other theories, for that matter).

As for predictions, very little should be said when a unique fit has not been found. Again, there is one positive statement that can be made from our experience--that is, if the P and P' choose the no-compensation mechanism, then a $\bar{p}p$ polarization prediction of around -50% near $t = -0.6\ (\mathrm{GeV}/c)^2$ seems unavoidable. Even though one can think of many ways of avoiding this (e.g., through ω-ω' interference), all good fits with this ghost-killing mechanism--three-pole, four-pole, and five-pole--produced the same prediction. This is bothersome mainly because of a parallel which can be drawn with the Kp data. At $p_{lab} = 2.0$ to 3.0 GeV/c, pp and $\bar{p}p$ as well as K^+p and K^-p have positive polarization for $-t < 0.8\ (\mathrm{GeV}/c)^2$.[26] At $p_{lab} = 6.0$ GeV/c, the K^+p and K^-p polarizations are still both positive in that t range, and the $\bar{p}p$ data are also positive for $-t < 0.3\ (\mathrm{GeV}/c)^2$. Hence one might expect the $\bar{p}p$ polarization to remain positive for $t = -0.6\ (\mathrm{GeV}/c)^2$, as does the K^-p. If it should remain positive, we would face a drastic contradiction to all of the parameterizations in which the P' vanishes near $t = -0.6\ (\mathrm{GeV}/c)^2$. Fits in which the Gell-Mann mechanism was used (fit #3 in Table IV) could predict positive $\bar{p}p$ polarization in that region, but this is apparently in contradiction to the CMSR results[21] on the P' ghost-killing mechanism. Obviously, data in this region are needed to settle the question.

ACKNOWLEDGMENTS

We wish to thank Professor Geoffrey F. Chew and the Lawrence Radiation Laboratory for their hospitality. One of the authors (D.M.A.) wishes to thank the U. S. Atomic Energy Commission for support, and another (W.H.G.) wishes to thank the Air Force Office of Scientific Research and National Research Council for support. Also, the authors thank Professor G. Bellettini for providing some preliminary data.

REFERENCES

1. William Rarita, Robert J. Riddell, Charles B. Chiu, and Roger J. N. Phillips, Phys. Rev. 165, 1615 (1967), hereafter referred to as RRCP.
2. J. V. Allaby, Yu. B. Bushnin, S. P. Denisov, A. N. Diddens, R. W. Dobinson, S. V. Donskov, G. Giacomelli, Yu. P. Gorin, A. Klovnin, A. I. Petrukhin, Yu. D. Prokoshkin, R. S. Shuvalov, C. A. Stahlbrand, and D. A. Stoyanova, Phys. Letters 30B, 500 (1969).
3. G. G. Beznogikh, A. Buyak, K. I. Iovchev, L. F. Kirillova, P. K. Markov, B. A. Morozov, V. A. Nikitin, P. V. Nomokonov, M. G. Shafranova, V. A. Sviridov, Troung Bien, V. I. Zayachki, N. K. Zhidkov, L. S. Zolin, S. B. Nurushev, and V. L. Solovianov, Phys. Letters 30B, 274 (1969).
4. D. Birnbaum, R. M. Edelstein, N. C. Hien, T. J. McMahon, J. F. Mucci, J. S. Russ, E. W. Anderson, E. J. Bleser, H. R. Blieden, G. B. Collins, D. Garelick, J. Menes, and F. Turkot, Phys. Rev. Letters 23, 663 (1969).
5. J. V. Allaby, F. Binon, A. N. Diddens, P. Duteil, A. Klovning, R. Meunier, J. P. Peigneux, E. J. Sacharidis, K. Schlupmann, M. Spighel, J. P. Street, A. M. Thorndike, and A. M. Wetherell, Phys. Letters 28B, 67 (1968).
6. M. Borghini, L. Dick, L. di Lella, A. Navarro, J. C. Olivier, K. Reibel, G. Coignet, D. Cronenberger, G. Gregoire, K. Kuroda, A. Michalowicz, M. Poulet, D. Sillou, C. Bellettini, P. L. Braccini, T. Del Prette, L. Foa, G. Sanguinetti, and M. Valdata, Phys. Letters 31B, 405 (1970).

7. R. T. Bell, M. Borghini, L. Dick, G. Gregoire, L. di Lella, J. C. Olivier, M. Poulet, P. Scharff-Hansen, D. Cronenberger, K. Kuroda, A. Michalowicz, G. Bellettini, P. L. Braccini, T. Del Prette, L. Foa, G. Sanguinetti, and M. Valdata, 14th International Conference on High Energy Physics, Vienna, ed. by J. Prentki and J. Steinberger (CERN, Geneve, 1968).

8. R. A. Carrigan, Phys. Rev. Letters 24, 168 (1970).

9. Most of these data are included in semiretrievable form in the compendium by Geoffrey C. Fox and Chris Quigg, Compilation of Elastic Scattering Data, Lawrence Radiation Laboratory Report UCRL-20001, Jan. 1970.

10. K. J. Foley, S. J. Lindenbaum, W. A. Love, S. Ozaki, J. J. Russel, and L. C. L. Yuan, Phys. Rev. Letters 11, 425, 503 (1963); ibid 15, 45 (1965).

11. W. Galbraith, E. W. Jenkins, T. F. Kycia, B. A. Leontic, R. H. Phillips, A. L. Read, and R. Rubenstein, Phys. Rev. 138, B913 (1965).

12. K. J. Foley, R. S. Jones, S. J. Lindenbaum, W. A. Love, S. Ozaki, E. D. Platner, C. A. Quarles, and E. H. Willen, Phys. Rev. Letters 19, 857 (1967).

13. G. Bellettini, G. Cocconi, A. N. Diddens, E. Lillethun, J. Pahl, J. P. Scanlon, J. Walters, A. M. Wetherell, and P. Zanella, Phys. Letters 14, 164 (1965).

14. P. Grannis, J. Arens, O. Chamberlain, B. Dieterle, C. Shultz, G. Shapiro, H. Steiner, L. Van Rossum, and D. Weldon, Phys. Rev. 148, 1297 (1966).

15. M. Borghini, G. Coignet, L. Dick, K. Kuroda, L. di Lella, P. C. Macq, A. Michalowicz, and J. C. Olivier, Phys. Letters 24B, 77 (1966).

16. E. Lohrmann, H. Meyer, and H. Winzler, Phys. Letters 13, 78 (1964).

17. A. E. Taylor, A. Ashmore, W. S. Chapman, D. F. Falla, W. H. Range, D. B. Scott, A. Astbury, F. Copocci, and T. G. Walker, Phys. Letters 14, 54 (1965).

18. G. Bellettini, G. Cocconi, A. N. Diddens, E. Lillethun, J. P. Scanlon, and A. M. Wetherell, Phys. Letters 19, 705 (1966).

19. Ling-Lie C. Wang, Phys. Rev. 142, 1187 (1966).

20. By "canonical" trajectories we mean those which are linear and pass through the particles on a Chew-Frautschi plot. "Canonical" residue functions are those which best satisfy the CMSR and FESR for KN and πN.

21. V. Barger and R. J. N. Phillips, Phys. Rev. 187, 2210 (1969).

22. G. V. Dass and C. Michael, Phys. Rev. 175, 1774 (1968).

23. A. P. Contogouris, J. Tran Thanh Van, and H. J. Lubatti, Phys. Rev. Letters 19, 1352 (1967).

24. P. di Vecchia, F. Drago, and M. Paciello, Nuovo Cimento 55A, 809 (1968).

25. G. V. Dass, C. Michael, and R. J. N. Phillips, Nucl. Phys. B9, 549 (1969).

26. C. Daum, F. C. Erne, J. P. Lagnaux, J. C. Sens, M. Steuer, and F. Udo, Nucl. Phys. B6, 617 (1968).

FIGURE CAPTIONS

Fig. 1. pp and $\bar{p}p$ differential cross sections compared with three pole fit number 2 of Table I, with predictions to 1800 GeV/c. Successive sets of data are spaced by a decade.

Fig. 2. $\bar{p}p$ polarization at 6 GeV/c compared with three pole fit number 2 of Table I and a prediction at 14 GeV/c.

Fig. 3. pp polarization at (a) 5.9, (b) 6, (c) 7, (d) 10, (e) 12, and (f) 14 GeV/c compared with three pole fit number 2 of Table I.

Fig. 4. Three pole fit number 2 of Table I compared with

(a) slope of pp differential cross section,

(b) total cross sections for pp and $\bar{p}p$,

(c) the ratio of the real to imaginary part of the forward scattering amplitude for pp, and

(d) the ratio of the real to imaginary part of the forward scattering amplitude for $\bar{p}p$.

Fig. 5. pp and $\bar{p}p$ differential cross sections compared with four pole fit number 2 of Table II, with predictions to 1800 GeV/c. Successive sets of data are spaced by a decade.

Fig. 6. $\bar{p}p$ polarization at 6 GeV/c compared with four pole fit number 2 of Table II and a prediction at 14 GeV/c.

Fig. 7. pp polarization at (a) 5.9, (b) 6, (c) 7, (d) 10, (e) 12, and (f) 14 GeV/c compared with four pole fit number 2 of Table II.

Fig. 8. Four pole fit number 2 of Table II compared with

(a) slope of pp differential cross section,

(b) total cross sections for pp and $\bar{p}p$,

(c) the ratio of the real to imaginary part of the forward scattering amplitude for pp, and

(d) the ratio of the real to imaginary part of the forward scattering amplitude for $\bar{p}p$.

Fig. 9. pp and $\bar{p}p$ differential cross sections compared with five pole fit number 1 of Table IV, with predictions to 1800 GeV/c. Successive sets of data are spaced by a decade.

Fig. 10. $\bar{p}p$ polarization at 6 GeV/c compared with five pole fit number 1 of Table IV and a prediction at 14 GeV/c.

Fig. 11. pp polarization at (a) 5.9, (b) 6, (c) 7, (d) 10, (e) 12, and (f) 14 GeV/c compared with five pole fit number 1 of Table IV.

Fig. 12. Five pole fit number 1 of Table IV compared with

(a) slope of pp differential cross section,

(b) total cross sections for pp and $\bar{p}p$,

(c) the ratio of the real to imaginary part of the forward scattering amplitude for $\bar{p}p$, and

(d) the ratio of the real to imaginary part of the forward scattering amplitude for pp.

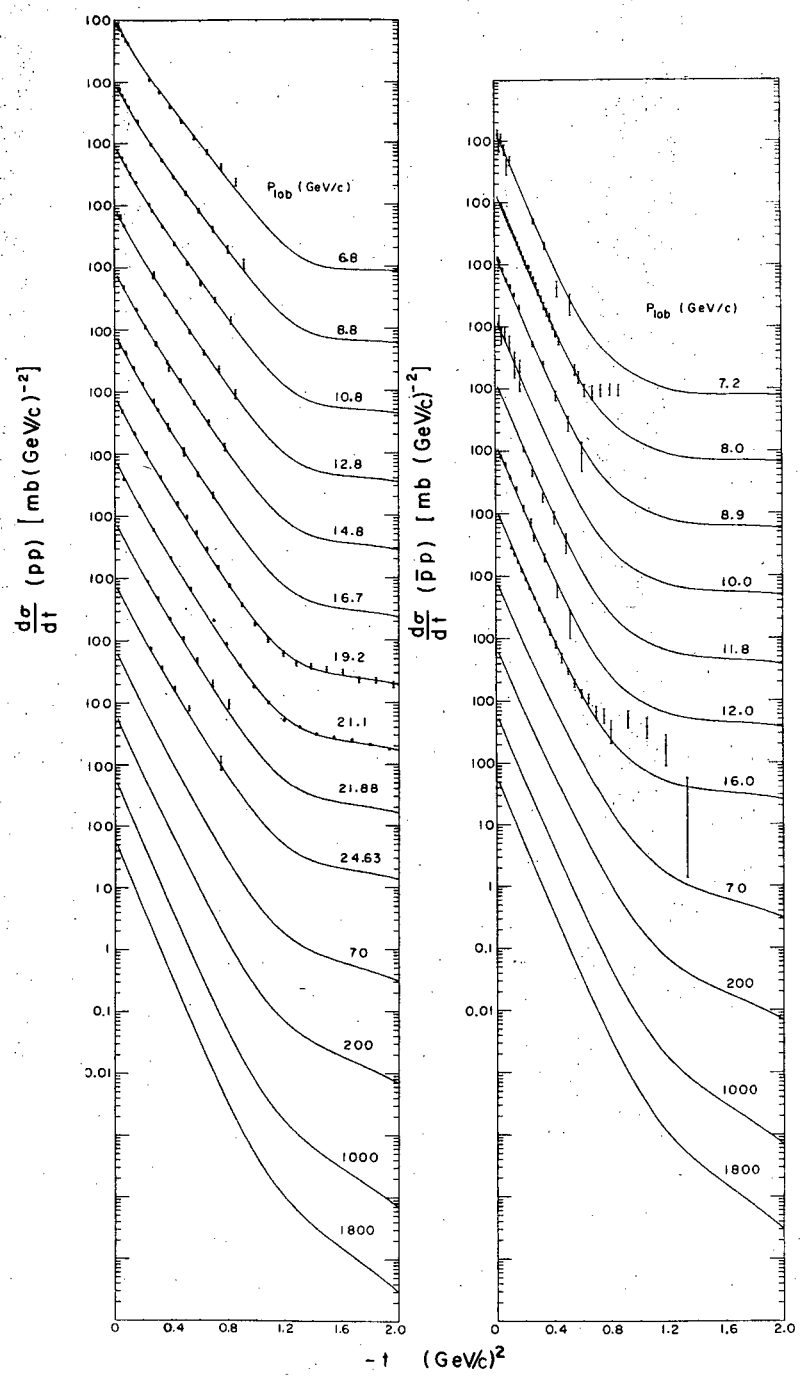
P_{lab} (GeV/c)
6.8
8.8
10.8
12.8
14.8
16.7
19.2
21.1
21.88
24.63
70
200
1000
1800
$\frac{d\sigma}{dt}$ (pp) [mb(GeV/c)$^{-2}$]
P_{lab} (GeV/c)
7.2
8.0
8.9
10.0
11.8
12.0
16.0
70
200
1000
1800
$\frac{d\sigma}{dt}$ ($\bar{p}$p) [mb (GeV/c)$^{-2}$]
-t (GeV/c)^2
XBL 705-2947

Fig. 1

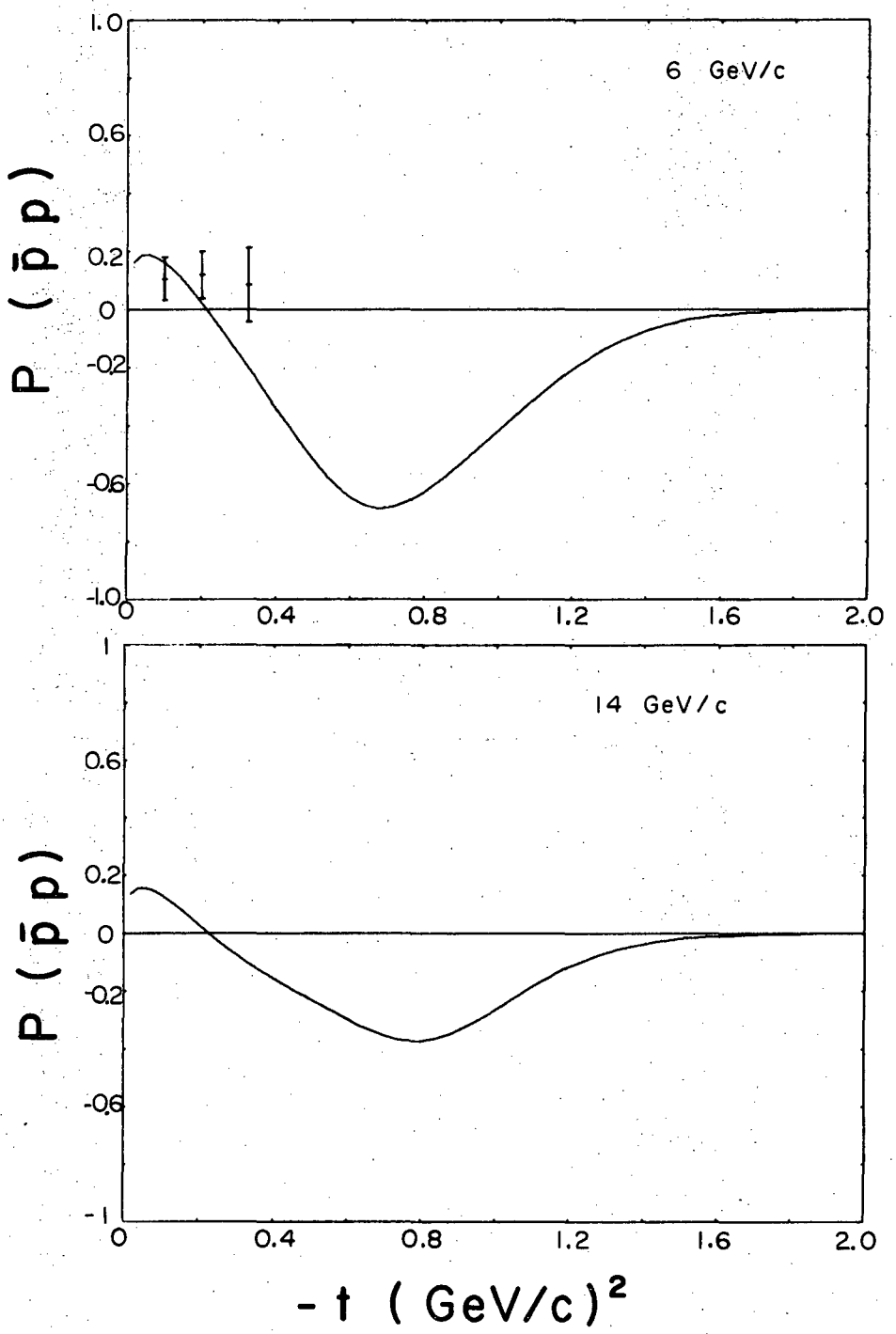

XBL 705 - 2968

Fig. 2

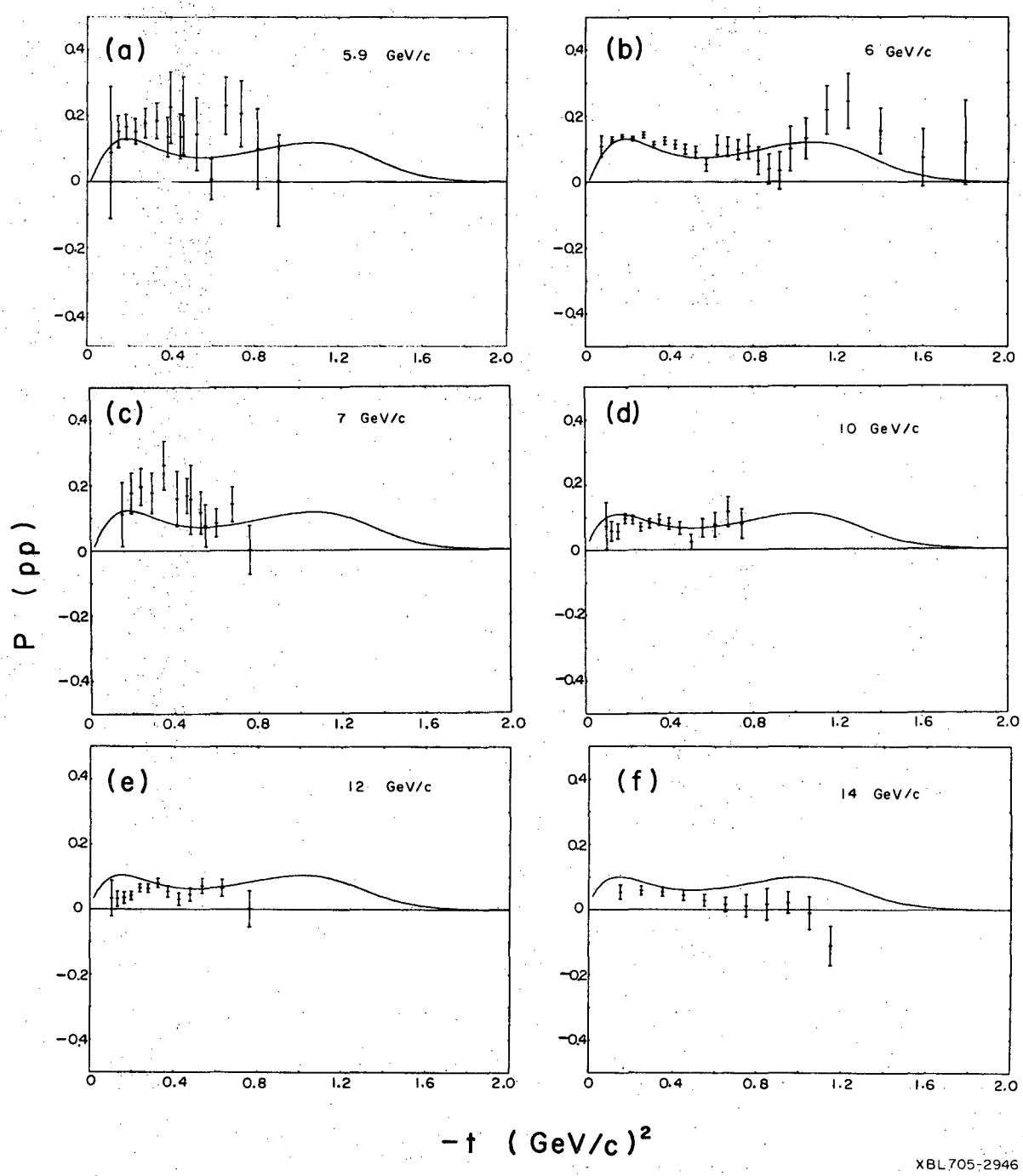
(a)
5.9 GeV/c
(b)
6 GeV/c
(c)
7 GeV/c
(d)
10 GeV/c
(e)
12 GeV/c
(f)
14 GeV/c
P (pp)
-t (GeV/c)²
XBL 705-2946

Fig. 3

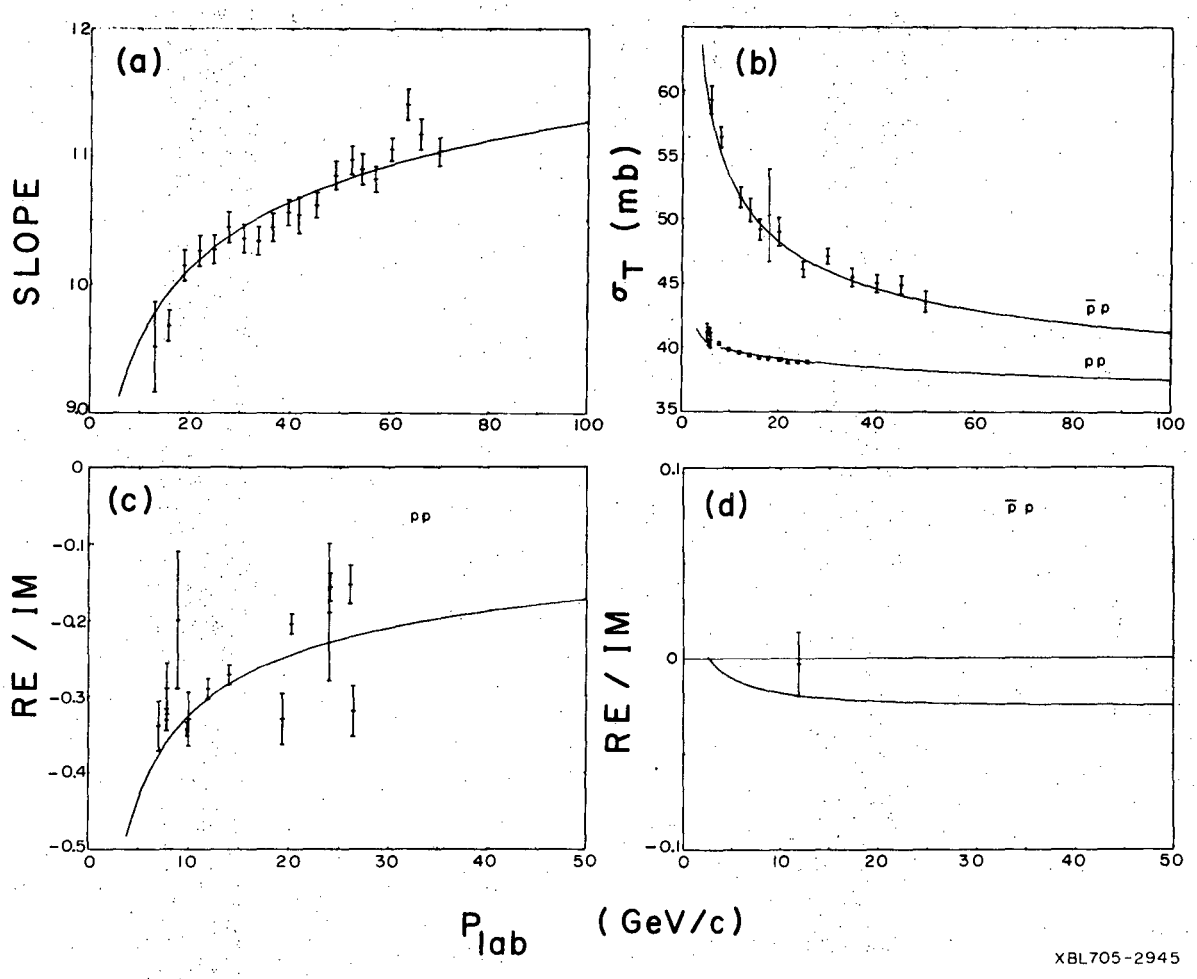
(a)
SLOPE
(b)
σ_T (mb)
$\bar{p}p$
pp
(c)
pp
RE / IM
(d)
$\bar{p}p$
RE / IM
P_{lab} (GeV/c)
XBL705-2945

Fig. 4

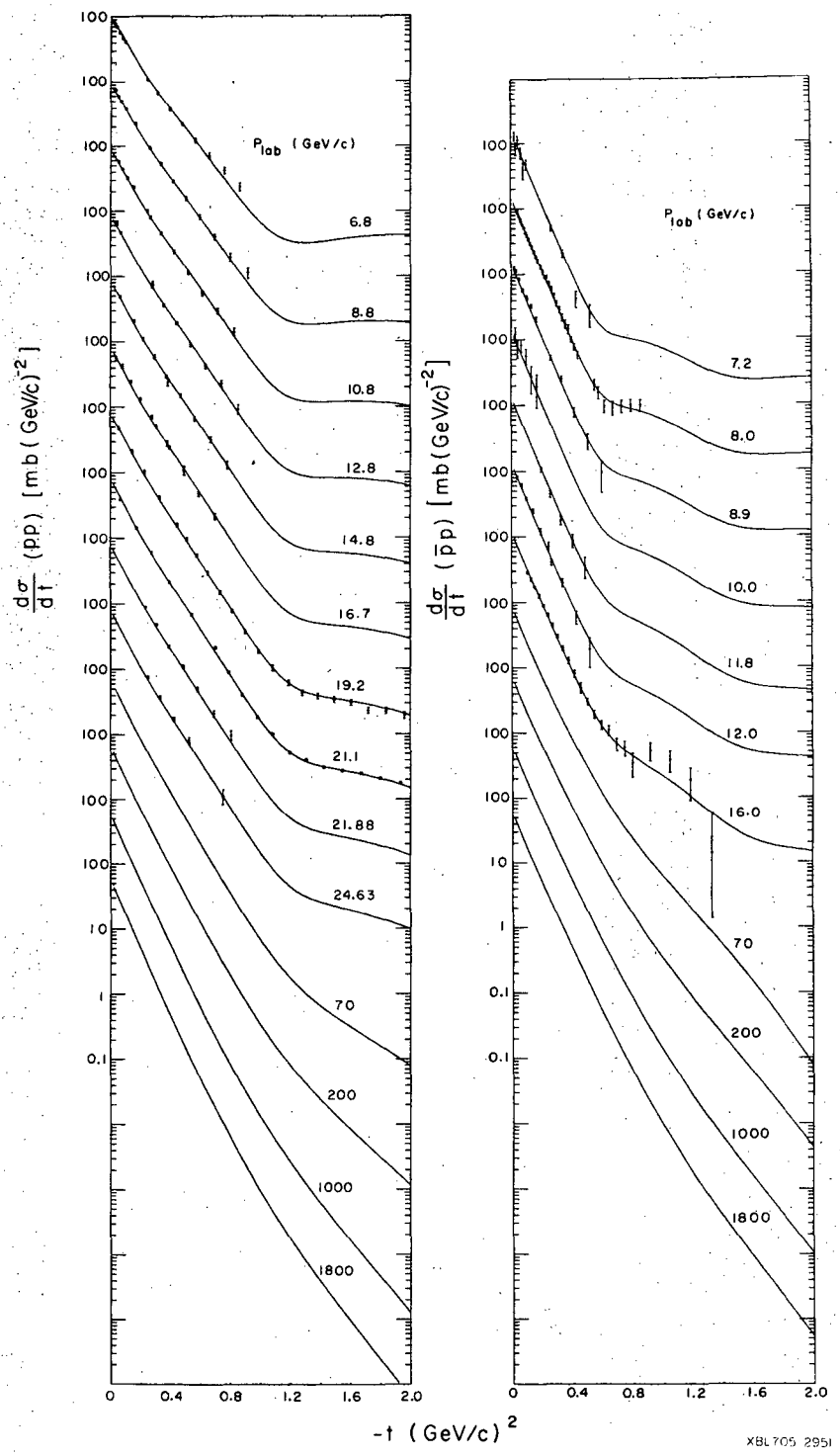
P_{lab} (GeV/c)
6.8
8.8
10.8
12.8
14.8
16.7
19.2
21.1
21.88
24.63
70
200
1000
1800
$\frac{d\sigma}{dt}$ (pp) [mb (GeV/c)$^{-2}$]
P_{lab} (GeV/c)
7.2
8.0
8.9
10.0
11.8
12.0
16.0
70
200
1000
1800
$\frac{d\sigma}{dt}$ ($\bar{p}$p) [mb (GeV/c)$^{-2}$]
-t (GeV/c)^2
XBL705 2951

Fig. 5

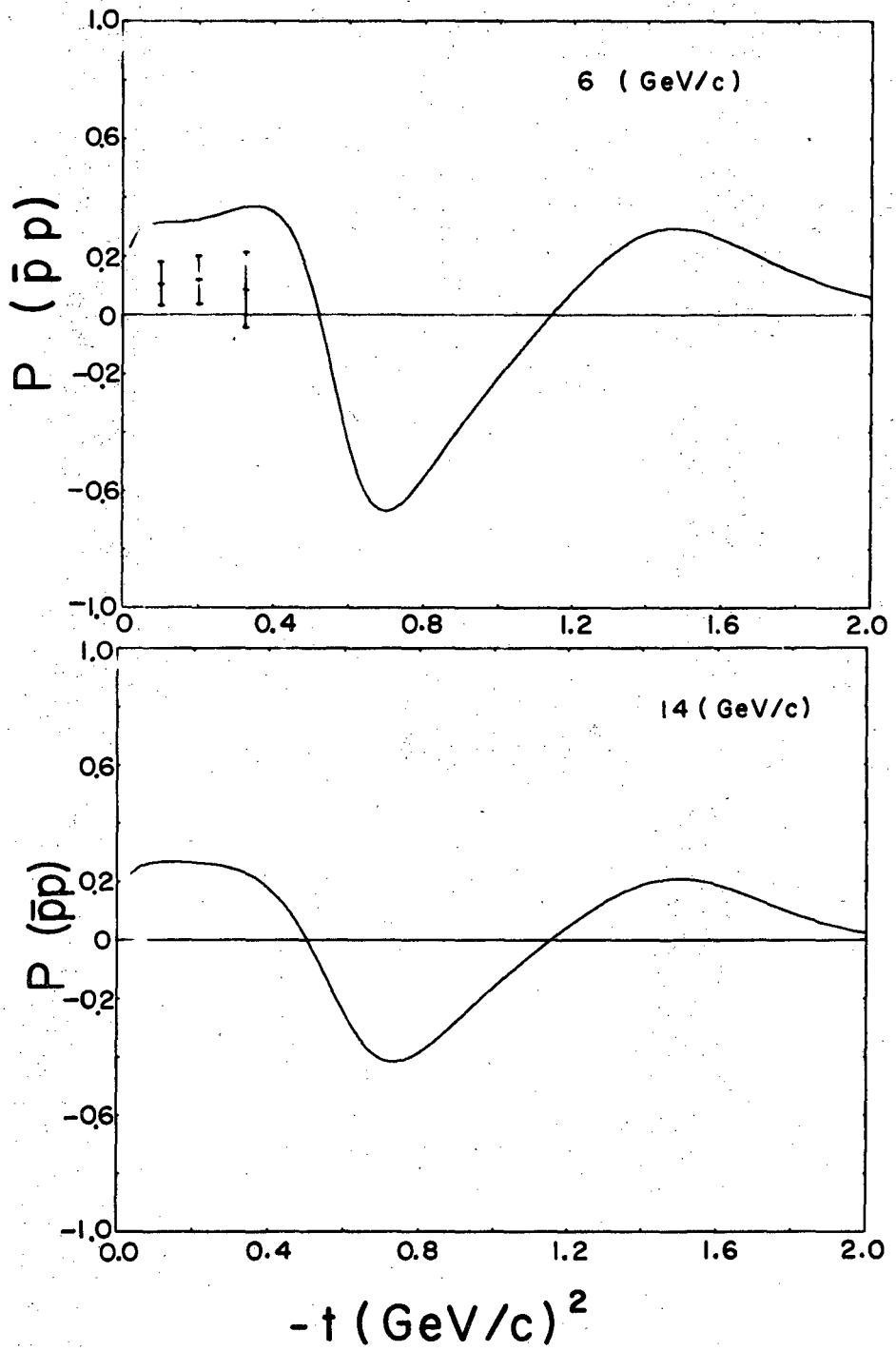

XBL705-2966

Fig. 6

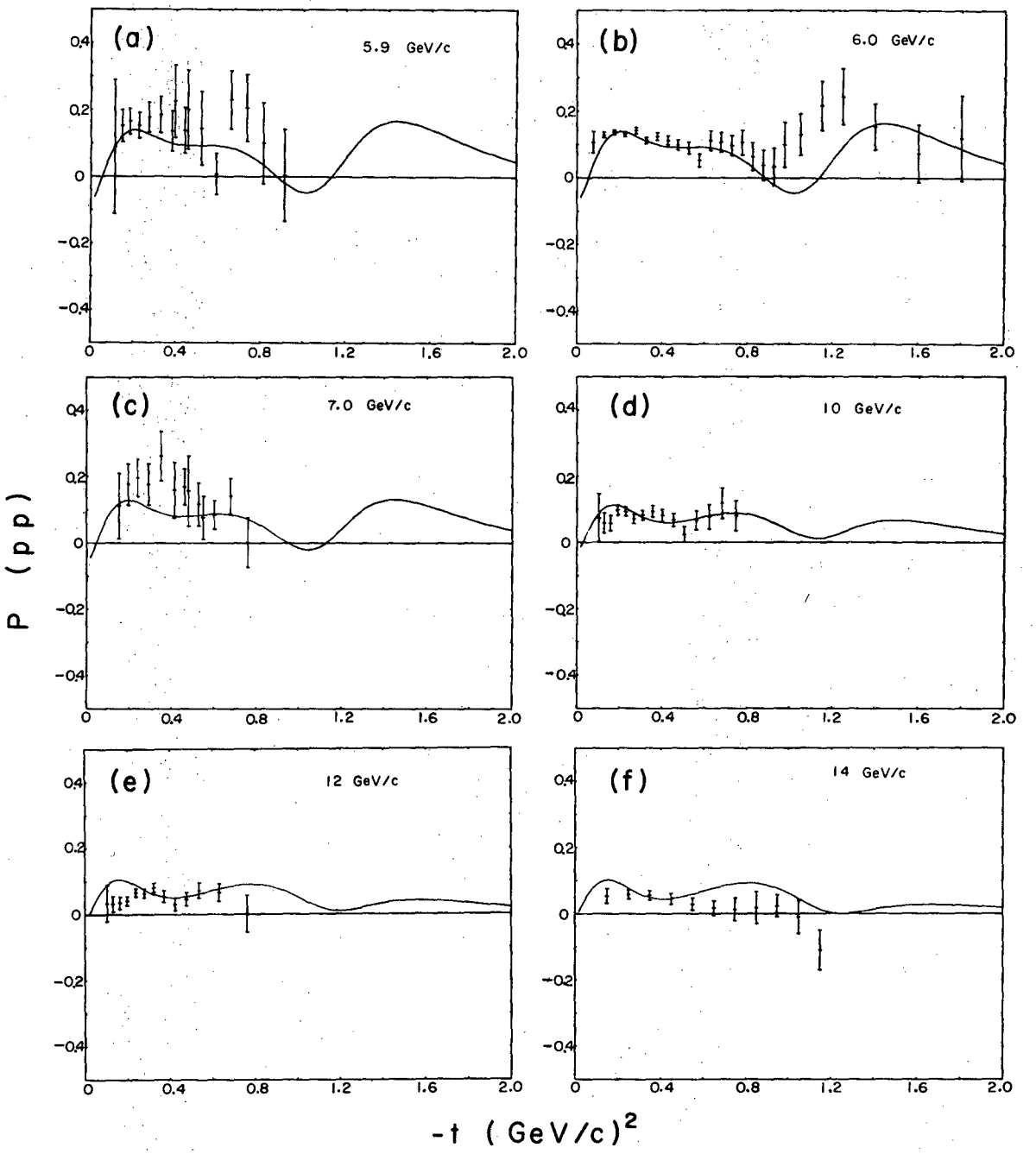

XBL705-2949

Fig. 7

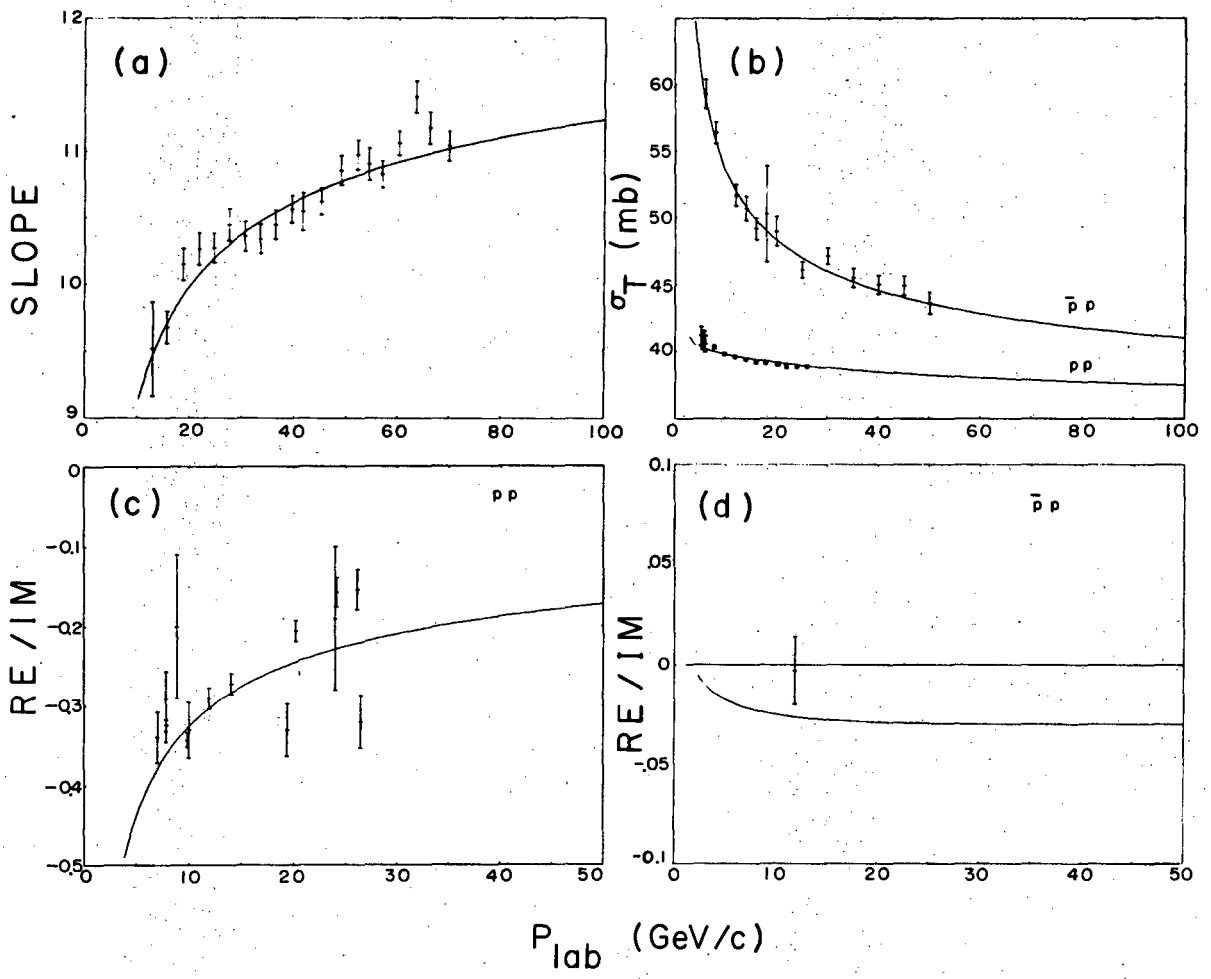

XBL705-2953

Fig. 8

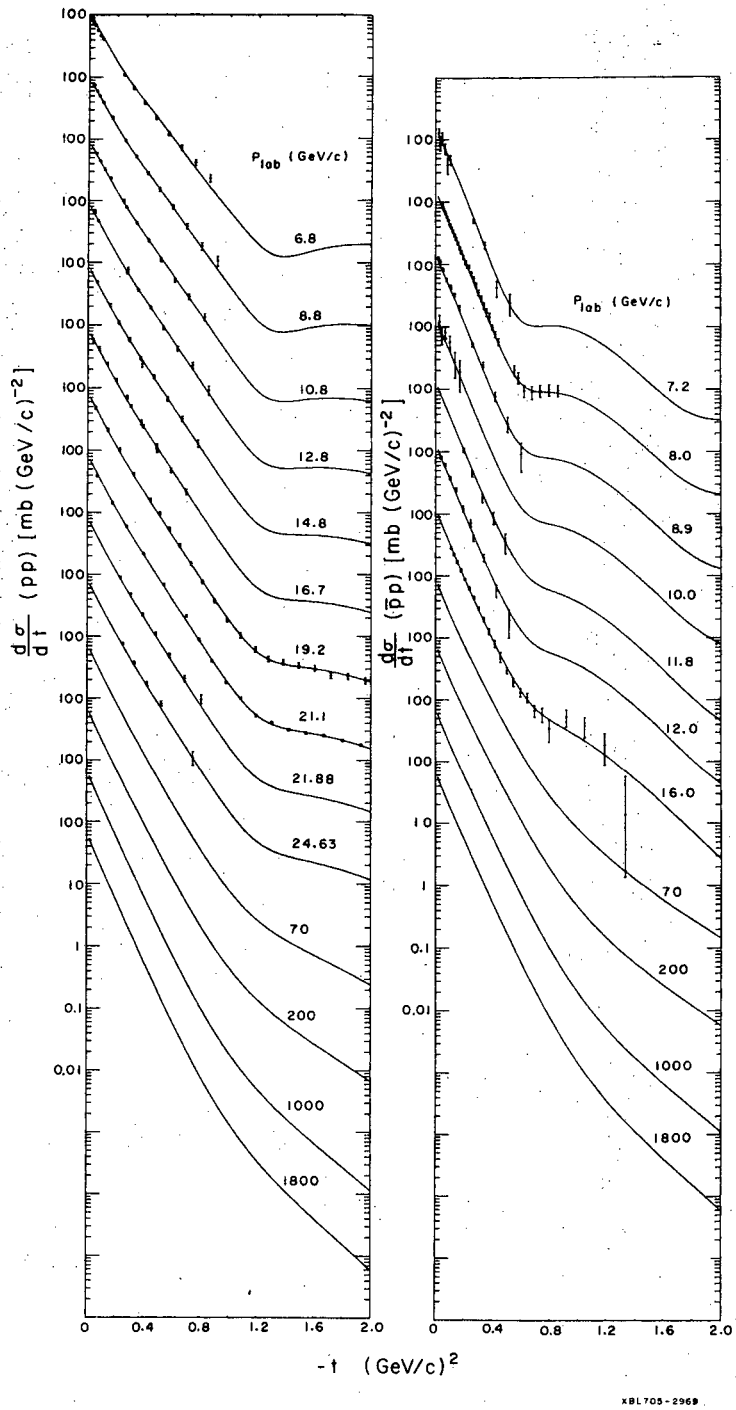
P_{lab} (GeV/c)
6.8
8.8
10.8
12.8
14.8
16.7
19.2
21.1
21.88
24.63
70
200
1000
1800
$\frac{d\sigma}{dt}$ (pp) [mb (GeV/c)$^{-2}$]
P_{lab} (GeV/c)
7.2
8.0
8.9
10.0
11.8
12.0
16.0
70
200
1000
1800
$\frac{d\sigma}{dt}$ ($\bar{p}p$) [mb (GeV/c)$^{-2}$]
-t (GeV/c)^2
XBL705-2969

Fig. 9

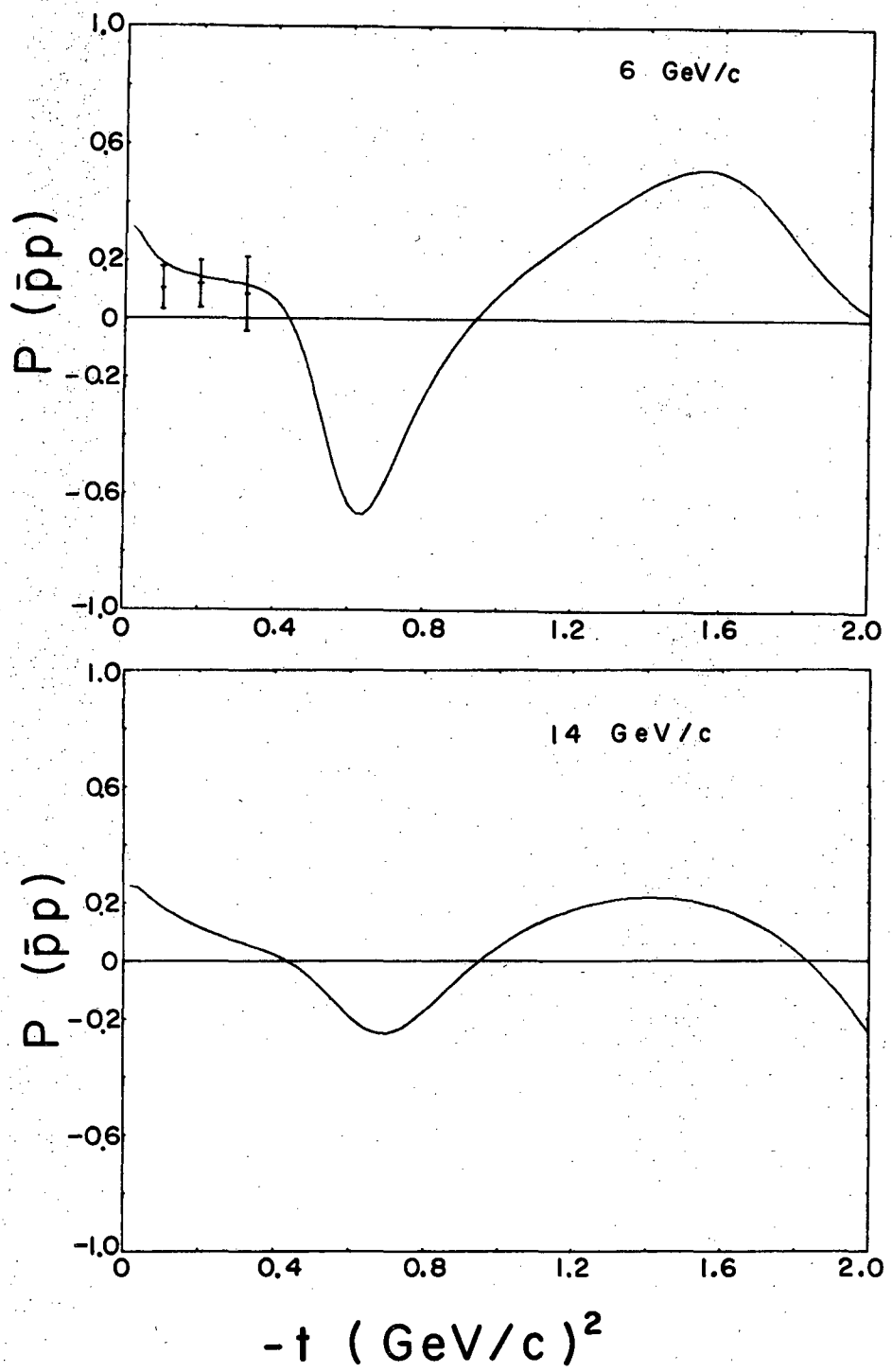

XBL705-2967

Fig. 10

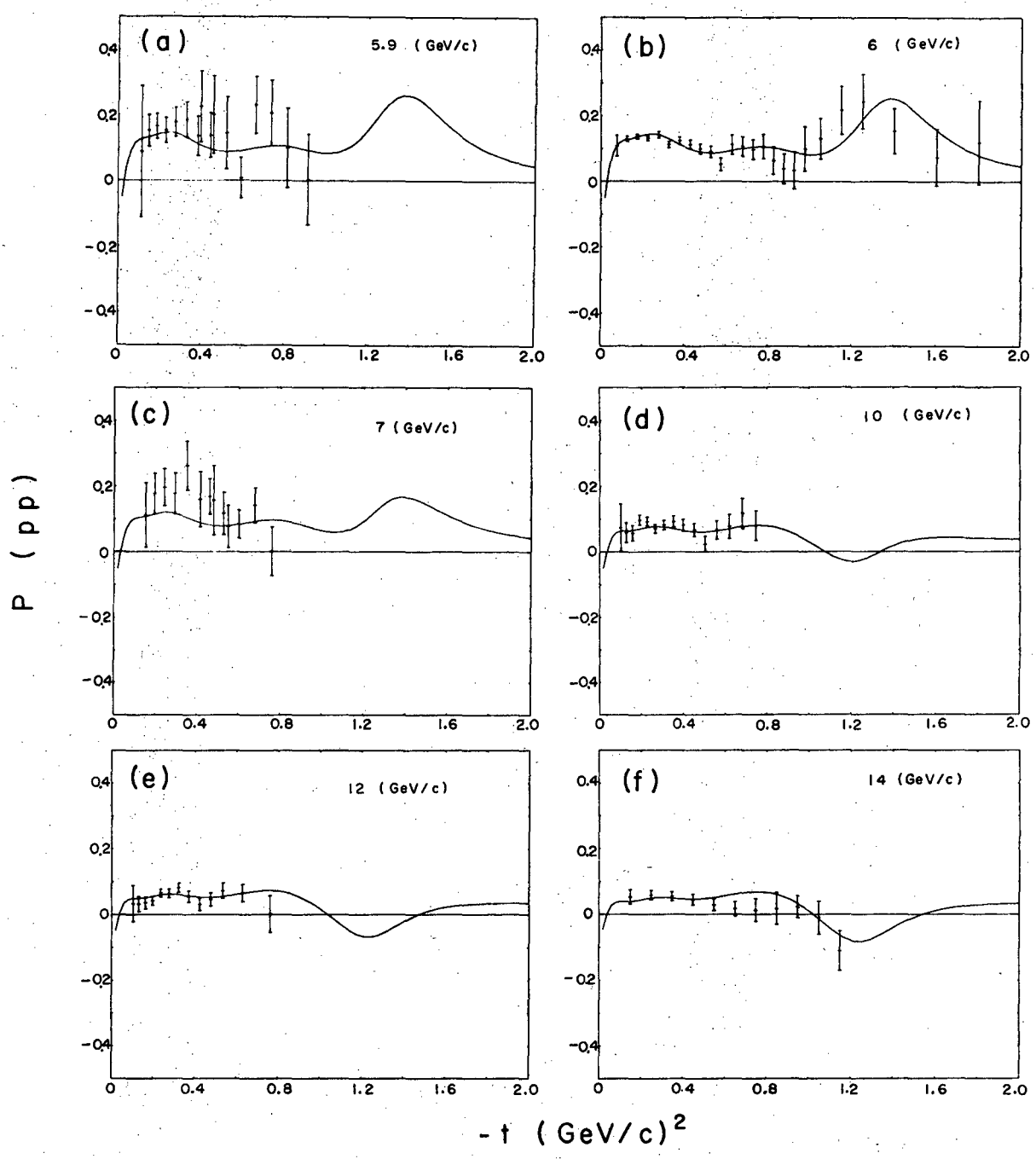

XBL705-2950

Fig. 11

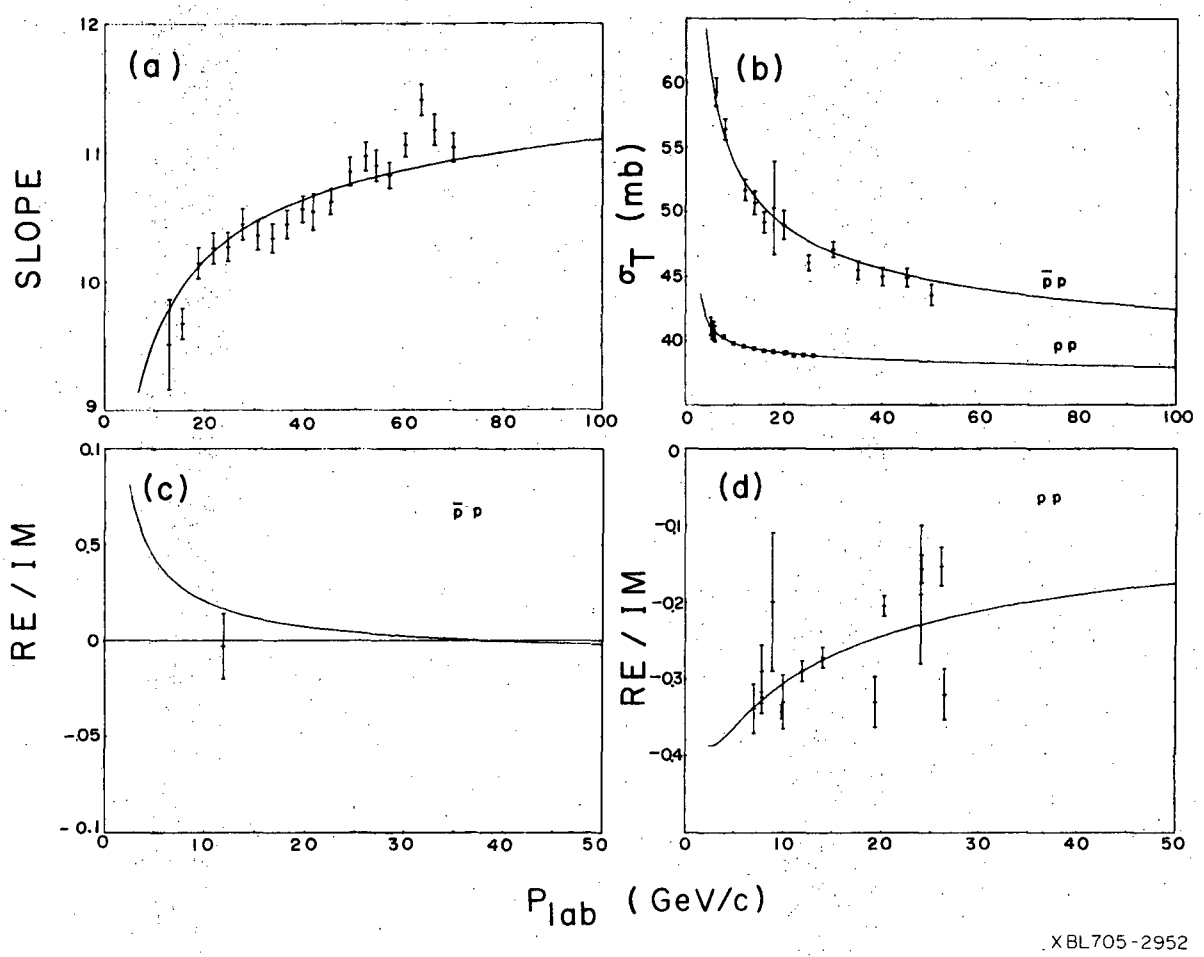
(a)
SLOPE
(b)
σ_T (mb)
$\bar{p}p$
pp
(c)
$\bar{p}p$
RE / IM
(d)
pp
RE / IM
P_{lab} (GeV/c)
XBL705-2952

Fig. 12

LEGAL NOTICE

This report was prepared as an account of Government sponsored work. Neither the United States, nor the Commission, nor any person acting on behalf of the Commission:

A. Makes any warranty or representation, expressed or implied, with respect to the accuracy, completeness, or usefulness of the information contained in this report, or that the use of any information, apparatus, method, or process disclosed in this report may not infringe privately owned rights; or

B. Assumes any liabilities with respect to the use of, or for damages resulting from the use of any information, apparatus, method, or process disclosed in this report.

As used in the above, "person acting on behalf of the Commission" includes any employee or contractor of the Commission, or employee of such contractor, to the extent that such employee or contractor of the Commission, or employee of such contractor prepares, disseminates, or provides access to, any information pursuant to his employment or contract with the Commission, or his employment with such contractor.

TECHNICAL INFORMATION DIVISION
LAWRENCE RADIATION LABORATORY
UNIVERSITY OF CALIFORNIA
BERKELEY, CALIFORNIA 94720